Progress In Electromagnetics Research C, Vol. 133, 181–194, 2023

Predictive Current Control of Permanent Magnet Synchronous Motor Based on Parameter Identification

Chengmin Wang* **and Aiyuan Wang**

Abstract—Aiming at the unsatisfactory accuracy and speed of traditional parameter identification methods for permanent magnet synchronous motors (PMSMs), a parameter identification method based on an improved hunter prey optimization (HPO) algorithm (Tent chaotic initialization and firefly algorithm HPO (TF-HPO)) was proposed. Using the Tent chaotic map, the initial individuals are evenly distributed to enrich their diversity, and the population position is updated using the firefly perturbation algorithm. Simulation and practical experiments show that compared with unmodified algorithm, the improved algorithm has faster convergence speed and higher recognition accuracy, and can effectively identify the parameters of the motor. On this basis, deadbeat predictive current control is implemented, effectively eliminating current static errors and improving the accuracy and stability of the current control system, and can effectively suppress motor torque ripple and current harmonics caused by parameter deviations.

1. INTRODUCTION

Permanent magnet synchronous motor (PMSM) is favored by all walks of life due to its advantages such as small size, light weight, high power factor, and good speed regulation. The vector control strategy, direct torque control strategy, and other control methods have been proposed and gradually applied to permanent magnet synchronous motors, further improving the control effect of permanent magnet synchronous motors. For example, deadbeat predictive current control has been widely used in many fields due to its fast dynamic response and ease of digital implementation, such as three-phase inverter control, induction motor current control [1], three-phase permanent magnet synchronous motor torque control [2], BOOST converter control [3], DC microgrid hybrid energy storage system control [4], single-phase pulse width modulation (PWM) inverter control [5], and five-phase permanent magnet synchronous motor current control [6]. Therefore, the research and application of motor control systems must master the relevant parameters of motor objects, such as motor stator resistance, AC/DC axis inductance, and permanent magnet magnetic linkage. Due to the influence of working environment and operation status, motor parameters will vary with factors such as temperature rise and magnetic field saturation during motor operation. However, changes in motor parameters can affect the performance of the control system, reduce system reliability, and may lead to unexpected control states.

Therefore, how to quickly and accurately identify the key parameters of PMSM has gradually become one of the hot research directions to improve the stability of PMSM systems. In recent years, scholars have combined advanced intelligent algorithms with parameter identification problems to improve the accuracy of parameter identification in response to the shortcomings of traditional parameter identification methods. Reference [7] mentions an identification method based on an improved sparrow search algorithm. By adding a new algorithm, the accuracy of the algorithm is improved while ensuring convergence accuracy. Reference [8] proposes an improved identification method for

Received 29 March 2023, Accepted 25 May 2023, Scheduled 4 June 2023
* Corresponding author: Chengmin Wang (596825933@qq.com).
The authors are with the School of Electrical Engineering, Shanghai Dian Ji University, Shanghai, China.

model reference adaptive systems, which overcomes the inaccuracy of identification results caused by the under-ranking problem of the mathematical model of electrical machines by identifying multiple parameters in steps. Reference [9] proposes an improved identification method based on the Grey Wolf optimization algorithm, which has higher accuracy and better stability than the unmodified algorithm. Reference [10] proposes an improved ant lion algorithm identification method, which improves the local optimization ability of the algorithm and greatly improves the accuracy and speed of parameter identification. Reference [11] proposes a parameter identification method based on an improved particle swarm optimization algorithm. The authors have proved through experiments that the algorithm has high recognition accuracy and fast convergence speed, while retaining the accuracy and robustness of the algorithm. Reference [12] proposes a new predictive current control strategy with high parameter robustness, which improves the robustness of motor control systems. The deadbeat model predictive control strategy has fast dynamic response, but its control accuracy is affected by the motor model. However, when the control system encounters parameter mismatches, the system performance will be reduced. Reference [13] proposes a current predictive control method based on a fuzzy algorithm. This control strategy adjusts the weight coefficient of the compensation link in real time according to the operating state of the motor and the mismatch of the controller's model parameters. This method can improve the control performance when the model parameters do not match. Reference [14] introduces the methods and results of comprehensive comparison between predictive current control and predictive torque control techniques in permanent magnet synchronous motors, and analyzes and compares the fluctuations in torque and stator flux, total harmonic distortion of input and output currents, and resonant characteristics of input filters. Reference [15] proposes a novel robust motion control system for permanent magnet synchronous motors based on wavelet neural networks. This control system combines the online learning ability of neural networks and the parameter identification ability of wavelet decomposition, improving the robustness of the system, while overcoming the influence of parameter uncertainties in the control drive process. However, the neural network algorithm has the problems of large computational load and long computational cycle, which limits the application scenarios of the algorithm. Reference [16] combines deadbeat current predictive control with this method. Firstly, based on the predictive equation of deadbeat current predictive control, a theoretically optimal voltage vector is calculated, and then an evaluation function is used to compare the voltage vector with the adjacent voltage vector. The one with the best evaluation function is selected as the control voltage of the inverter. Reference [17] proposes a multi-parameter online identification method that replaces a given voltage with a measured voltage, taking into account the under-ranking problem of the identification matrix. This method uses recursive least squares step-by-step identification to identify four parameters, namely, stator winding resistance, d-axis and q-axis inductances, and rotor permanent magnet flux linkage. However, the least square algorithm is susceptible to noise interference, which will reduce the accuracy of the identification results.

In this paper, a parameter identification method based on improved HPO algorithm (TF-HPO) is proposed, and on this basis, predictive current control for PMSM is implemented. Compared to other algorithms, this algorithm has faster convergence speed, higher accuracy, and higher parameter identification accuracy, resulting in higher accuracy of motor predictive current control.

This paper consists of five sections. In the second section, the mathematical model of PMSM and the deadbeat current predictive control model are established, and the principle of motor parameter identification is presented. In the third section, the HPO algorithm and optimization process are expounded. In the fourth section, the differences between the algorithms are compared through standard functions, and the advantages of predictive current control based on improved parameter identification algorithm are verified through simulation and experiments. In the fifth section, the research results of this article are summarized.

2. DEADBEAT PREDICTIVE CURRENT CONTROL MODEL

2.1. PMSM Mathematical Model

The mathematical model of permanent magnet synchronous motor in three-phase static coordinate system is relatively complex, and corresponding coordinate transformation is required to simplify

its mathematical model. To establish a permanent magnet synchronous motor model, the following assumptions are often made:

(i) Ignore motor core saturation.

(ii) Ignore eddy current losses and hysteresis losses.

(iii) The back electromotive force of the motor is a sine wave.

(iv) The rotor does not have a damping winding.

Based on the above assumptions, the stator voltage equation of PMSM in synchronous rotating coordinate system is obtained, as shown in Equation (1):

$$\begin{cases} \dfrac{di_d}{dt} = -\dfrac{R_s}{L_d} i_d + \dfrac{L_q}{L_d} \omega_e i_q + \dfrac{u_d}{L_d} \\ \dfrac{di_q}{dt} = -\dfrac{R_s}{L_q} - \dfrac{L_d}{L_q} \omega_e i_d + \dfrac{u_q}{L_q} - \dfrac{\psi_f}{L_q} \omega_e \end{cases} \tag{1}$$

where u_d, u_q, i_d, i_q, L_d, L_q are the voltage, current, and inductance of the d and q axes, respectively; R_s is the stator resistance; ψ_f is the permanent magnet magnetic chain; ω_e is the electrical angular velocity of the rotor.

2.2. Deadbeat Predictive Current Control Model

The principle of predictive current control algorithm is to predict the motor current at the next moment based on the discrete mathematical models of the motor and inverter, and accurately control the motor current in a very short time. Therefore, the dynamic response speed of the current loop is fast, and the motor current harmonics are small, which makes the motor torque and servo system have excellent control effect and good response speed. In addition, the concept of predictive current control is simple and intuitive, and the control algorithm is easy to implement.

Deadbeat current control originates from discrete linear state feedback control, which allows the feedback current to track a given current for a limited time. Its principle is to compare the motor current obtained by over sampling with the given current through coordinate transformation. The comparison result is controlled by a deadbeat current controller, and the output voltage is subjected to coordinate transformation. Then, an inverter switching pulse signal is generated through the space vector PWM (SVPWM). Compared with traditional current controllers, proportional-integral (PI) controllers are replaced by deadbeat controllers, which have the advantages of constant switching frequency, fast dynamic response, high bandwidth, small current fluctuations, and easy implementation.

According to the voltage equation, select the motor current as the state variable, and when the motor is a surface mounted permanent magnet synchronous motor, the motor inductance L_d=L_q=L, then the state space function is obtained, as shown in Equation (2):

$$\frac{d}{dt}\begin{bmatrix} i_d \\ i_q \end{bmatrix} = \begin{bmatrix} -\dfrac{R_s}{L} & \omega_e \\ -\omega_e & -\dfrac{R_s}{L} \end{bmatrix} \begin{bmatrix} i_d \\ i_q \end{bmatrix} + \begin{bmatrix} \dfrac{1}{L} & 0 \\ 0 & \dfrac{1}{L} \end{bmatrix} \begin{bmatrix} u_d \\ u_q \end{bmatrix} + \begin{bmatrix} 0 \\ -\dfrac{\omega_e \psi_f}{L} \end{bmatrix} \tag{2}$$

And rewrite this equation into the form of a standard state space function, as shown in Equation (3):

$$\dot{x} = Ax + Bu + D \tag{3}$$

where $x = \begin{bmatrix} i_d \\ i_q \end{bmatrix}$ $u = \begin{bmatrix} u_d \\ u_q \end{bmatrix}$ $A = \begin{bmatrix} -\frac{R_s}{L} & \omega_e \\ -\omega_e & -\frac{R_s}{L} \end{bmatrix}$ $B = \begin{bmatrix} \frac{1}{L} & 0 \\ 0 & \frac{1}{L} \end{bmatrix}$ $D = \begin{bmatrix} 0 \\ -\frac{\omega_e \psi_f}{L} \end{bmatrix}$.

In permanent magnet synchronous motor control systems, the current sampling period is relatively short. The first order Taylor equation is used to discretize the current state equation, and the differential term of the original current state equation can be approximated as shown in Equation (4):

$$\begin{cases} \dfrac{di_d}{dt} = \dfrac{i_d(k+1) - i_d(k)}{T_s} \\ \dfrac{di_q}{dt} = \dfrac{i_q(k+1) - i_q(k)}{T_s} \end{cases} \tag{4}$$

where T_s is the current sampling period; $i_d(k)$, $i_q(k)$, $i_d(k+1)$, $i_q(k+1)$ are the sampling value of the d-axis and q-axis current at the k and $k+1$ moments of the motor, respectively. The discretized current prediction equation for permanent magnet synchronous motors can be obtained by bringing Equation (4) into Equation (3), as shown in Equation (5):

$$\begin{bmatrix} i_d(k+1) \\ i_q(k+1) \end{bmatrix} = F(k) \cdot \begin{bmatrix} i_d(k) \\ i_q(k) \end{bmatrix} + G \cdot \begin{bmatrix} u_d(k) \\ u_q(k) \end{bmatrix} + H(k) \tag{5}$$

where $F(k) = \begin{bmatrix} 1 - \frac{T_s R_s}{L} & T_s \omega_e(k) \\ -T_s \omega_e(k) & 1 - \frac{T_s R_s}{L} \end{bmatrix}$, $G = \begin{bmatrix} \frac{T_s}{L} & 0 \\ 0 & \frac{T_s}{L} \end{bmatrix}$, $H(k) = \begin{bmatrix} 0 \\ -\frac{T_s \omega_e(k) \psi_f}{L} \end{bmatrix}$.

Deadbeat predictive current control is a type of predictive current control, characterized in that the given current of the system is taken as the current of the system at the next moment, so as to achieve the output current of the system to keep up with the given current at the next moment. In order to achieve a deadbeat of the system current, the predicted currents of d-axis $i_d(k+1)$ and q-axis $i_q(k+1)$ at the moment $k+1$ in Equation (5) are replaced by the given d-axis current $i_d^*(k)$ and q-axis current $i_q^*(k)$ of the system, to obtain the reference voltage at this time, as shown in Equation (6):

$$\begin{bmatrix} u_d(k) \\ u_q(k) \end{bmatrix} = G^{-1} \left(F(k) \cdot \begin{bmatrix} i_d(k) \\ i_q(k) \end{bmatrix} - \begin{bmatrix} i_d^*(k) \\ i_q^*(k) \end{bmatrix} + H(k) \right) \tag{6}$$

2.3. Principle of Parameter Identification

Parameter identification of permanent magnet synchronous motor is an inverse problem, which is to determine the required parameters based on experimental data and established models. According to the voltage equation, the parameters to be identified include stator resistance, stator inductance, and permanent magnet flux linkage. The voltage equation is a two-dimensional equation set, so the equation set lacks rank, and the solution is not unique, resulting in inability to accurately identify the three parameters. According to research, the influence of deviation of resistance parameters on predictive current control can be negligible [18]. Therefore, this paper only identifies the inductance and flux linkage parameters of the motor, so that the equations are fully ranked.

Design a model with the same structure and adjustable parameters based on the reference model of the motor, as shown in Equation (7):

$$\frac{d}{dt} \begin{bmatrix} \hat{i}_d \\ \hat{i}_q \end{bmatrix} = \begin{bmatrix} -\frac{R_s}{\hat{L}_S} & \omega_e \\ -\omega_e & -\frac{R_s}{\hat{L}_S} \end{bmatrix} \begin{bmatrix} \hat{i}_d \\ \hat{i}_q \end{bmatrix} + \begin{bmatrix} \frac{1}{\hat{L}_S} & 0 \\ 0 & \frac{1}{\hat{L}_S} \end{bmatrix} \begin{bmatrix} u_d \\ u_q \end{bmatrix} + \begin{bmatrix} 0 \\ -\frac{\omega_e(k) \hat{\psi}_f}{\hat{L}_S} \end{bmatrix} \tag{7}$$

where $\hat{L}_s \hat{\Psi}_f$ is the parameter to be identified, and $\hat{i}_d$ and $\hat{i}_q$ are the stator voltage input on the dq axis of the actual PMSM model.

Using an objective function to evaluate both outputs, the parameter identification algorithm continuously adjusts the model parameters. Repeat the above process until the fitness value reaches the minimum, and the identified parameter L can be considered. $\hat{L}_s \hat{\Psi}_f$ is equivalent to the theoretical motor model parameters. The fitness function is defined as shown in Equation (8):

$$f\left(\hat{L}_s, \hat{\Psi}_f\right) = \sum_{k=1}^{n} \left(i_d(k) - \hat{i}_d(k)\right)^2 + \left(i_q(k) - \hat{i}_q(k)\right)^2 \tag{8}$$

The schematic diagram of parameter identification is shown in Figure 1.

3. TF-HPO ALGORITHM

3.1. Hunter Prey Optimization Algorithm

Hunter prey optimization algorithm is a novel swarm intelligence optimization algorithm proposed by Naruei et al. in 2022 [19]. Inspired by the fact that hunters attack individuals far away from the prey

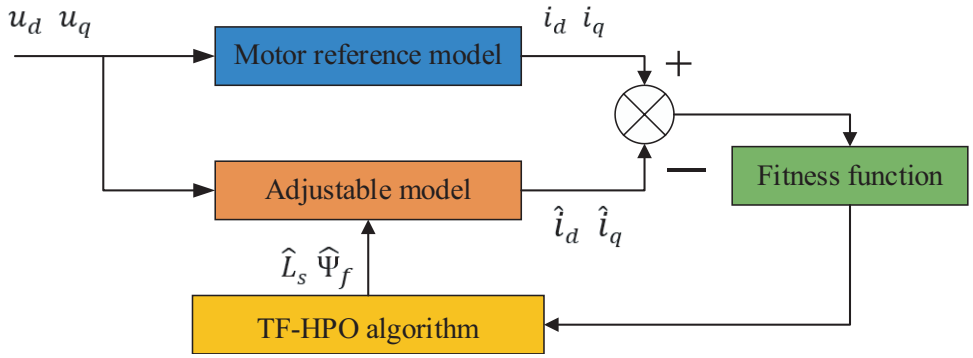

Figure 1. The flowchart of the TF-HPO algorithm.

population and constantly adjust their position by referring to the average population position of the prey. At the same time, the prey will constantly adjust its position, making itself tend to a safer position.

3.1.1. Initialize Population Members

Set them to $(\vec{x}) = \{\vec{x}_1,\vec{x}_2,\ldots,\vec{x}_n\}$. The objective function of the members in the population is expressed as $\vec{O} = \{O_1, O_2,\ldots,O_n\}$; position of each member i is randomly generated in the search space; the equation is as follows:

$$x_i{=}rand\,(1{,}d) * (ub{-}lb) + lb \tag{9}$$

where x_i is the location of the prey, lb the minimum value (lower bound) of the problem variable, ub the maximum value (upper bound) of the problem variable, and d the number (dimension) of the problem variable.

3.1.2. Predator Search Strategy

Hunters often choose prey that is far away from the group as their hunting target, which tends to be highly random. The equation for updating the hunter's position is as follows:

$$x_{i,j}\,(t+1) = x_{i,j}\,(t) + 0.5\left[\left(2CZP_{pos(j)} - x_{i,j}\,(t)\right) + \left(2\,(1-C)\,Z\cdot\gamma\,(j) - x_{i,j}\,(t)\right)\right] \tag{10}$$

where $x_{i,j}(t)$ is the current position of the predator, $x_{i,j}(t{+}1)$ the updated location of the predator, P_{pos} the location of the prey, $\gamma(j)$ the average of all locations, Z an adaptive parameter, and C a balance parameter between exploration and development. The calculation equation for C, Z, and $\gamma(j)$ are as follows:

$$C = 1 - \omega\left(\frac{0.98}{\omega_{\max}}\right) \tag{11}$$

$$P = \vec{R}_1 < C \tag{12}$$

$$U = (P == 0) \tag{13}$$

$$Z = R_2 \otimes U + \vec{R}_3 \otimes (\sim U) \tag{14}$$

$$\gamma = \frac{1}{n}\sum_{i=1}^{n}\vec{x}_i \tag{15}$$

where ω is the current number of iterations, and $\omega_{\max}$ is the maximum number of iterations. $\vec{R}_1$ and $\vec{R}_3$ are random vectors within the range of $[0, 1]$; R_2 is a random number; P is a random vector related to the number of variables; and U is the index value of the vector $\vec{R}_1$ that satisfies the condition $(P == 0)$.

In order to solve the convergence delay caused by considering the maximum distance between members and the average position in each iteration, a decreasing mechanism is introduced, and the equation for calculating the prey position is:

$$\vec{P}_{pos} = \vec{x}_i | a \ is \ sorted \ D_{euc}\left(k_{best}\right), \quad k_{best} = round\left(C \times N\right) \tag{16}$$

where $D_{euc}(k)$ is the Euclidean distance from the average position of each member, k_{best} a decreasing mechanism, and N the number of search agents.

3.1.3. Prey Escape Strategy

In the algorithm, when the prey is attacked, it will try to escape to a safe position, assuming that the safest position is the global best position, so that the prey can have a chance to survive. The equation for updating prey position is as follows:

$$x_{i,j}\left(t+1\right) = H_{pos} + C \cdot Z \cos\left(2\pi R_4\right) \times \left(H_{pos} - x_{i,j}\left(t\right)\right) \tag{17}$$

where H_{pos} is the globally optimal position, and R_4 is the random number in the range of $[-1, 1]$. The cos function locates the next prey position in the globally optimal position with different radials and angles, thus improving the performance in the development phase.

3.1.4. The Choice between Hunter and Prey

In order to select hunter and prey, the corresponding selection mechanism is given by combining Equations (10) and (17), and the equation is as follows:

$$x_{i,j}\left(t+1\right) = \begin{cases} x_{i,j}\left(t\right) + 0.5\left[\left(2CZP_{pos(j)} - x_{i,j}\left(t\right)\right) + \left(2\left(1-C\right)Z \cdot \gamma\left(j\right) - x_{i,j}\left(t\right)\right)\right] & R_5 < \delta \quad (18a) \\ H_{pos} + C \cdot Z \cos\left(2\pi R_4\right) \times \left(H_{pos} - x_{\alpha,\beta}\left(t\right)\right) & R_5 \geq \delta \quad (18b) \end{cases}$$

where R_5 is a random number within the range of $[0, 1]$, and δ is an adjustment parameter.

3.2. Tent Chaotic Initialization

Due to good ergodic uniformity and convergence speed, Tent chaotic mapping is used to optimize the hunter-prey algorithm, and the equation is as follows:

$$Z_{i+1} = \begin{cases} 2 \cdot Z_{i+1} & 0 \leq Z_i \leq \dfrac{1}{2} \\ 2 \cdot \left(1 - Z_i\right) & \dfrac{1}{2} \leq Z_i \leq 1 \end{cases} \tag{19}$$

$$X_i = D_{\min} + \left(D_{\max} - D_{\min}\right) \cdot Z_i \tag{20}$$

where Z_i is the ith chaotic sequence; Z_1 is one dimensional vector composed of D numbers by uniform random number in $[0, 1)$; X_i is the location information of the ith hunter, where $i = 1, 2, \ldots, n$; $D_{\min}$ and $D_{\max}$ are the lower and upper bounds of the feasible region, respectively.

3.3. Firefly Algorithm

Firefly algorithm is a heuristic optimization algorithm inspired by nature [20]. The authors' inspiration comes from the flickering behavior of fireflies. The main purpose of firefly flash is as a signal system to attract other fireflies.

The hypothesis is: fireflies are gender neutral; each firefly will be attracted by the brighter firefly; and the attraction is proportional to their brightness. For any two fireflies, the less bright firefly is attracted, so it moves to the brighter one, but the brightness decreases with the increase of its distance. If a brighter firefly is not found, it will move randomly.

In the D-dimensional solution space, the position of each firefly is as follows:

$$X = (x_1, x_2 \ldots x_D) \tag{21}$$

The relative fluorescence brightness of fireflies is as follows:

$$I{=}I_0{\cdot}e^{-\gamma r_{i,j}} \tag{22}$$

where I_0 is the maximum fluorescent brightness of the firefly, which is related to the objective function value. The better the objective function value is, the higher its brightness is. γ is the light intensity absorption coefficient; the fluorescence will be gradually weakened with the increase of distance and the absorption of the media; $r_{i,j}$ is the spatial distance between fireflies i and j.

The relative attraction between fireflies is determined by the following equation:

$$\beta_{fa}{=}\beta_0{\cdot}e^{-\gamma r_{i,j}^2} \tag{23}$$

where β_0 is the maximum attraction.

The position update equation of firefly i attracted to firefly j is as follows:

$$X_i{=}X_i{+}\beta_{fa}\left(x_j{-}x_i\right){+}\alpha\cdot\left(Q{-}\frac{1}{2}\right) \tag{24}$$

where x_i and x_j are the spatial positions of fireflies i and j; $\alpha\in(0,1]$ is the step factor, which is taken as 0.4 in this paper; Q is a random number subject to uniform distribution in $[0,1]$.

3.4. Process of TF-HPO Algorithm

The flowchart of the TF-HPO algorithm is shown in Figure 2.

3.5. Parameter Identification Based on TF-HPO Algorithm

The system block diagram of predictive current control based on parameter identification is shown in Figure 3.

4. SIMULATION AND EXPERIMENTAL VERIFICATION

4.1. Algorithm Performance Test

In order to test the effectiveness of the improved algorithm, five standard test functions are selected to verify the improved algorithm, and compared with HPO algorithm, Particle Swarm Optimization (PSO) algorithm, Harris hawks optimization (HHO) algorithm, and Whale Optimization Algorithm (WOA). The first three functions are unimodal functions, and the last two functions are multimodal functions. The standard test function information is shown in Table 1. The results of algorithm optimization and comparison experiments are shown in Table 2. The best value, worst value, average value, and standard deviation of each algorithm in the test function are listed. Each algorithm will be run 20 times, with the average and standard deviation as evaluation criteria. The smaller the average and standard deviation are, the better the performance is.

Table 1. Standard test function.

Num.	Function	Dim.	Range	$F_{\min}$
1	$F_1(x)=\sum_{i=1}^{n}\left(\sum_{j=1}^{i}x_j\right)^2$	30	$[-100,100]$	0
2	$F_2(x)=\max\left\{\left\|x_i\right\|,1\le i\le n\right\}$	30	$[-100,100]$	0
3	$F_3\left(x\right)=\sum_{i=1}^{n}\left[100\left(x_{i+1}-x_i^2\right)^2+\left(x_i-1\right)^2\right]$	30	$[-30,30]$	0
4	$F_4\left(x\right)=-20\exp\left(-0.2\sqrt{\frac{1}{n}\sum_{i=1}^{n}x_i^2}\right)-\exp\left(\frac{1}{n}\sum_{i=1}^{n}\cos\left(2\pi x_i\right)\right)+20+e$	30	$[-32,32]$	0
5	$F_5\left(x\right)=\frac{1}{4000}\sum_{i=1}^{n}x_i^2-\prod_{i=1}^{n}cos\left(\frac{x_i}{\sqrt{i}}\right)+1$	30	$[-600,600]$	0

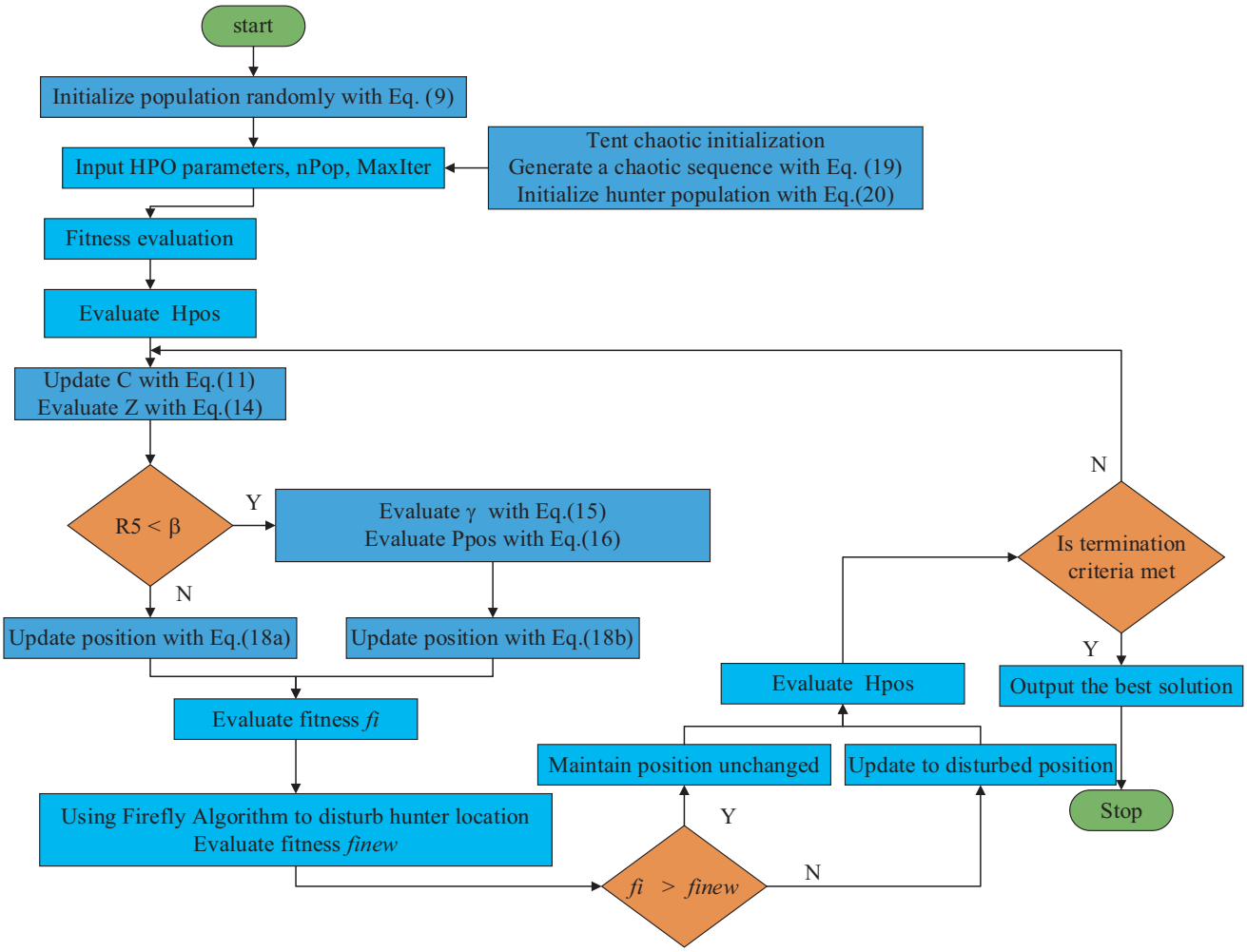

Figure 2. The flowchart of the TF-HPO algorithm.

4.2. Simulation Results and Analysis

In order to verify the performance of predictive current control based on TF-HPO algorithm, a simulation model was built in the MATLAB/SIMULINK environment. The motor parameters used are shown in Table 3.

The results and errors of each identification algorithm are shown in Table 4.

It can be seen from Table 4 that some of the basic algorithms compared are prone to falling into local optima, resulting in larger accuracy errors. After calculation, the maximum error rate of inductance parameter identification is 6.77%, and the maximum error rate of magnetic flux identification is 7.3%. However, the error rates of inductance and magnetic flux identification based on the improved TF-HPO algorithm are 2.1% and 1.9%, respectively, which reflects the advantages of the improved algorithm such as good robustness, high identification accuracy, fast convergence speed, and difficulty in falling into local optimal solutions.

Compare the dynamic response performance and steady-state performance of the system before and after adding the parameter identification module. The response of the current and rotational speed of the d axis and q axis of the system are shown in Figure 4 and Figure 5.

After powering on, the initial load of the given system is $0\,\mathrm{N}\cdot\mathrm{m}$, the initial rotational speed set to 1000rpm, and a step torque of $10\,\mathrm{N}\cdot\mathrm{m}$ applied at $0.2\,\mathrm{S}$. After adding the parameter identification algorithm, the system speed collapse is not obvious and has excellent resistance to load disturbances. The currents of d axis and q axis have a relatively large current ripple for an extremely short time when

Table 2. The results of algorithm optimization and comparison experiments.

Function		TF-HPO	HPO	PSO	HHO	WOA
F_1	worst	2.125e-144	0.0014177	1655.3088	1.9747e-73	77911.2649
	best	4.8337e-159	6.368e-09	144.4169	7.5816e-97	22160.2961
	avg	7.0978e-146	0.0001089	705.5008	7.3121e-75	49304.8815
	std	3.8795e-145	0.00027107	374.0712	3.6064e-74	13888.0351
F_2	worst	1.9138e-76	1.5538	9.222	4.1015e-48	90.8896
	best	4.679e-83	0.018393	2.6354	2.2482e-64	0.63375
	avg	2.0117e-77	0.3713	5.5958	2.8774e-49	48.1807
	std	5.0094e-77	0.3628	1.7375	8.865e-49	25.9539
F_3	worst	26.0057	32.6867	3265.9273	0.046694	28.7441
	best	23.1074	26.4304	395.2169	2.1425e-05	27.1566
	avg	23.6597	28.5989	1310.819	0.011778	27.9145
	std	0.56852	0.98266	709.752	0.013516	0.45396
F_4	worst	8.8818e-16	8.8818e-16	1.5447e-04	1.7918	8.8818e-16
	best	8.8818e-16	8.8818e-16	2.7383	14.2214	7.9936e-15
	avg	8.8818e-16	8.8818e-16	1.1543	5.7800	3.8488e-15
	std	0	0	0.8514	2.9934	2.8119e-15
F_5	worst	0	0	2.932e-07	0.0105	0
	best	0	0	0.2670	0.2054	0
	avg	0	0	0.031	0.0864	0
	std	0	0	0.0381	0.0375	0

Table 3. Main parameters of the motor.

parameter	**numerical value**
sampling period/s	10e-6
stator resistance/Ω	0.958
Q axis inductance L_q/mH	12
D axis inductance L_d/mH	12
flux linkage ψ_f/Wb	0.1827
number of pole pairs P_n	4
Rotational inertia $J/(\mathrm{kg}\cdot\mathrm{m}^2)$	0.003

Table 4. The results and errors of each identification algorithm.

Parameter	TF-HPO	HPO	PSO	HHO	WOA
Stator d-axis and q-axis inductance/mH	11.748	11.676	11.064	11.448	11.5908
Error/%	2.1	2.7	6.77	4.66	3.41
Permanent magnet flux linkage/Wb	0.17923	0.1766	0.1694	0.1741	0.1761
Error/%	1.9	3.4	7.3	4.7	3.6

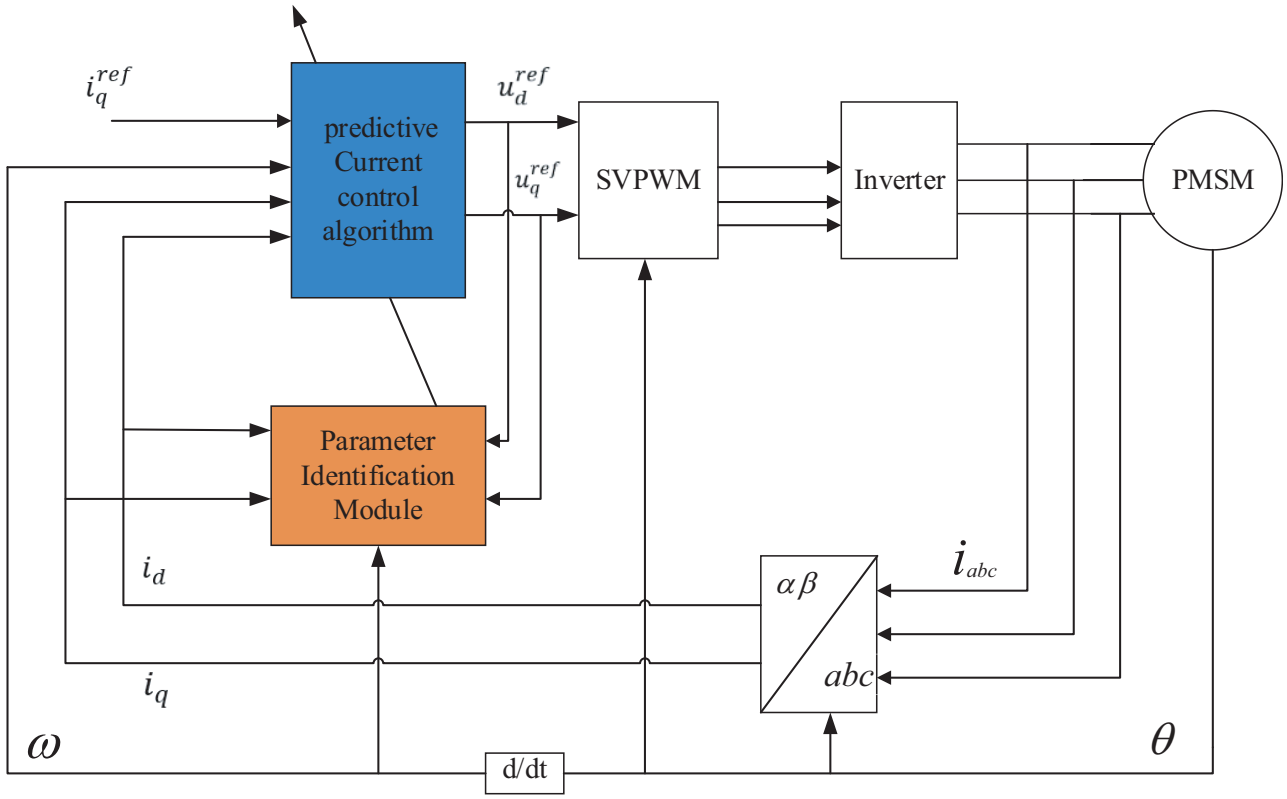

Figure 3. Block diagram of predictive current control based on parameter identification.

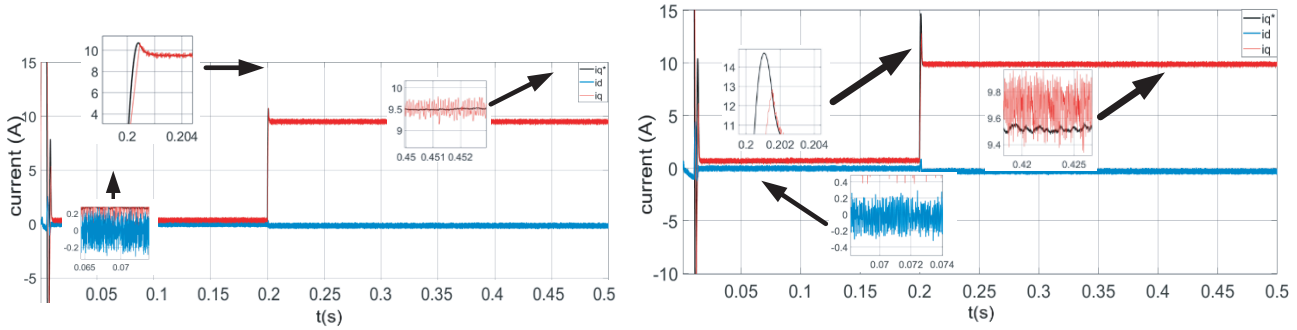

Figure 4. Current response. (a) Predictive current control with parameter identification. (b) Predictive current control without parameter identification.

the motor starts. This is because the parameter identification algorithm requires a certain convergence time, and the parameter fluctuation before convergence is large, resulting in an increase in current ripple. Subsequently, there is no static difference between the reference current and the response currents of the d axis and q axis, and the torque ripple is reduced.

4.3. Experimental Results and Analysis

In order to verify the effectiveness of this method, an experimental verification of the predictive current control method based on parameter identification is carried out on the experimental platform shown in Figure 6. The platform mainly includes a multifunctional digital signal processing (DSP) motor control

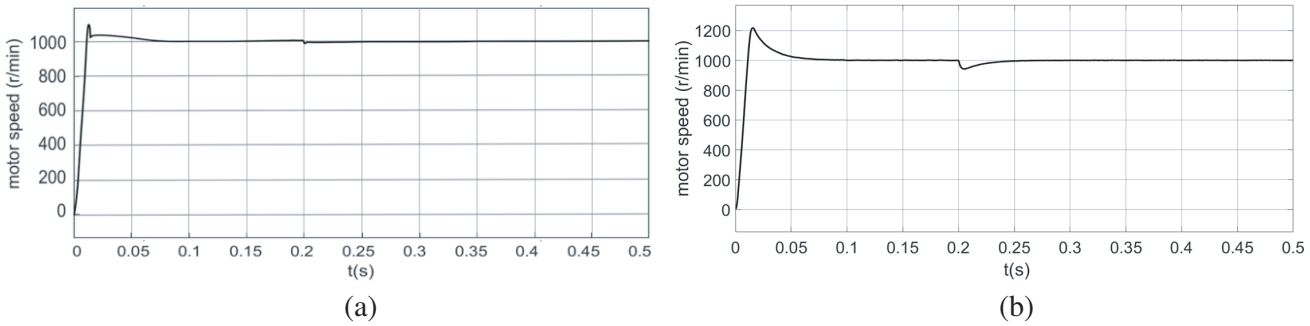

Figure 5. Motor speed. (a) Predictive current control with parameter identification. (b) Predictive current control without parameter identification.

driver board, an upper computer, a 24 V switching power supply, and a PMSM. The control chip of the driver board adopts TMS320F28335, and the power supply voltage of the control board is 24 V. The motor parameters used in this experiment are consistent with the simulation motor parameters. The identification results are shown in Figure 7.

By adding a parameter identification algorithm to the predictive current control experiment and comparing the output effects before and after adding the algorithm, considering that parameter changes have little impact on the rotational speed of the motor, only the steady-state current and torque waveforms are compared here. The experimental results are shown in Figure 8 and Figure 9.

As shown in Figure 8, by comparing the changes in the waveform of the A-phase current before and after the addition of the parameter identification algorithm, it can be seen that there is significant distortion in the motor phase current near the peak and valley, and the overall waveform is not smooth enough. After the addition of the parameter identification algorithm, the total harmonic content of the current is reduced from 17.34% to 9.72%. As shown in Figure 9, after adding an improved parameter identification algorithm module, the torque ripple under steady-state conditions was reduced from 1.3 N· m to 0.7 N · m, and the smoothness of the torque was improved, verifying the improvement effect of the parameter identification algorithm on the steady-state performance of the system in predictive current control.

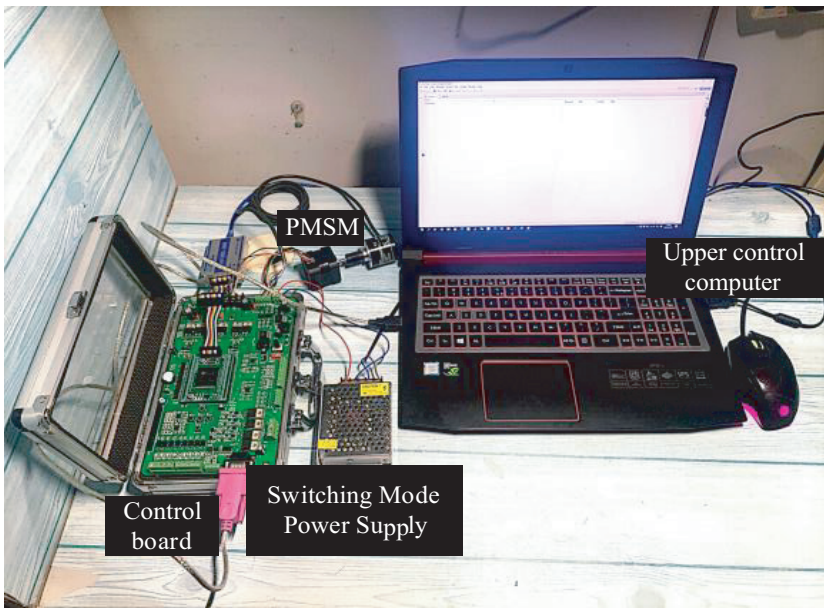

Figure 6. The experimental platform.

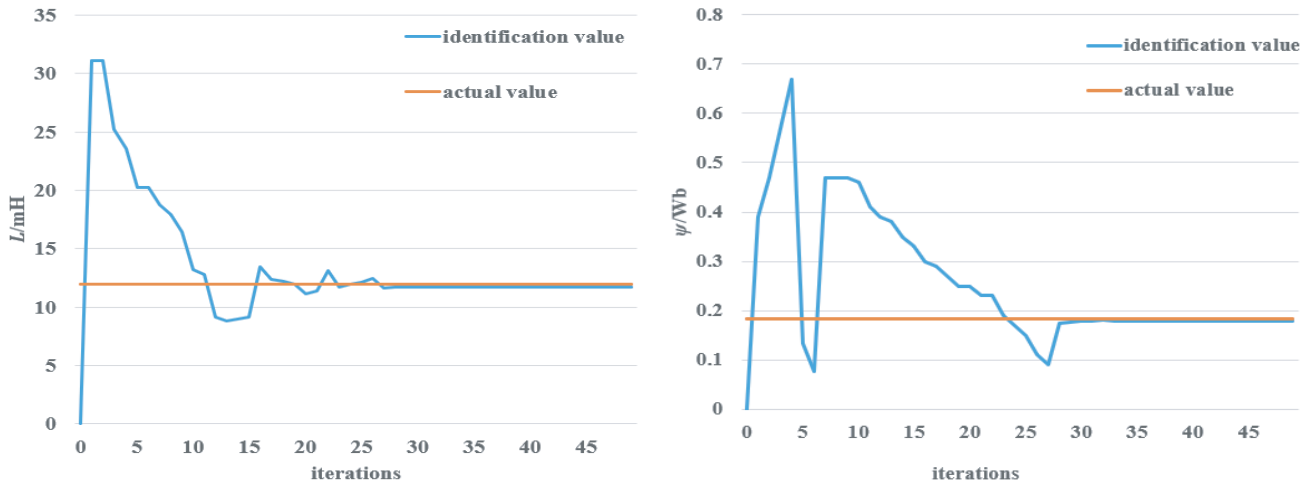

Figure 7. Results of parameter identification. (a) Parameter identification of inductance. (b) Parameter identification of magnetic linkage.

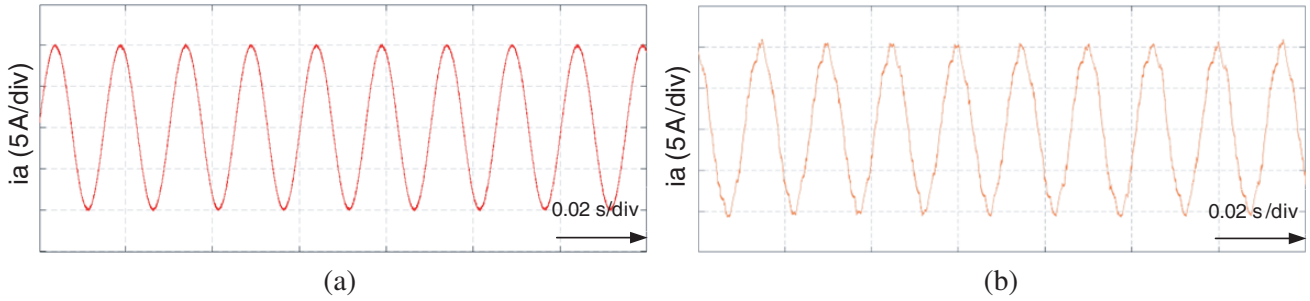

Figure 8. Experimental diagram of A-phase current. (a) Predictive current control with parameter identification. (b) Predictive current control without parameter identification.

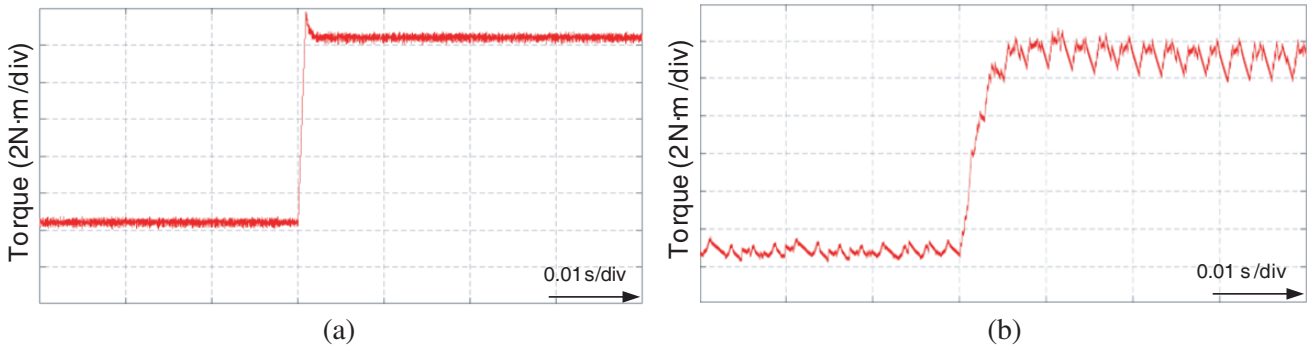

Figure 9. Experimental diagram of torque. (a) Predictive current control with parameter identification. (b) Predictive current control without parameter identification.

5. CONCLUSIONS

Due to the complexity and nonlinear nature of permanent magnet synchronous motor systems, it is difficult to obtain high-precision identification results using conventional methods due to the existence of local extremum points in the optimization function. This paper proposes a parameter identification method for permanent magnet synchronous motors based on an improved HPO algorithm, constructs a PMSM parameter identification model, and optimizes it using the improved HPO algorithm. The following conclusions have been drawn from the results obtained through simulation and experiments.

(i) In this paper, improvements were made to the HPO algorithm, and the superiority of the improved HPO algorithm over other algorithms was verified through standard function testing.

(ii) In this paper, a parameter identification model based on the improved HPO algorithm was established. Through experiments, it was found that the inductance identification error was only 2.1%, and the flux identification error was only 1.9%. Compared with parameter identification models under other algorithms, it was verified that the parameter identification model based on the TF-HPO algorithm has better robustness, faster convergence speed, and higher accuracy.

(iii) By adding a parameter identification module, the distortion of the phase current under predictive current control has been effectively improved. The total harmonic content of the current has decreased from 17.34% to 9.72%. The torque ripple of the motor has been reduced from $1.3\,\mathrm{N}\cdot\mathrm{m}$ to $0.7\,\mathrm{N}\cdot\mathrm{m}$, effectively suppressing torque ripple and current distortion caused by motor parameter deviations while improving the dynamic response performance of the system, with good control results.

REFERENCES

1. Wang, B., X. Chen, Y. Yu, et al., "Robust predictive current control with online disturbance estimation for induction machine drives," *IEEE Transactions on Power Electronics*, Vol. 32, No. 6, 4663–4674, 2016.
2. Wang, Y., X. Wang, W. Xie, et al., "Deadbeat model-predictive torque control with discrete space-vector modulation for PMSM drives," *IEEE Transactions on Industrial Electronics*, Vol. 64, No. 5, 3537–3547, 2017.
3. Wang, B., X. Zhang, and H. B. Gooi, "An SI-MISO boost converter with deadbeat-based control for electric vehicle applications," *IEEE Transactions on Vehicular Technology*, Vol. 67, No. 10, 9223–9232, 2018.
4. Wang, B., U. Manandhar, X. Zhang, et al., "Deadbeat control for hybrid energy storage systems in DC microgrids," *IEEE Transactions on Sustainable Energy*, Vol. 10, No. 4, 1867–1877, 2018.
5. Wang, P., Y. Bi, F. Gao, et al., "An improved deadbeat control method for single-phase PWM rectifiers in charging system for EVs," *IEEE Transactions on Vehicular Technology*, Vol. 68, No. 10, 9672–9681, 2019.
6. Saeed, M. S. R., W. Song, B. Yu, et al., "Low-complexity deadbeat model predictive current control with duty ratio for five-phase PMSM drives," *IEEE Transactions on Power Electronics*, Vol. 35, No. 11, 12085–12099, 2020.
7. Cao, Y., R. Mao, L. Feng, et al., "Multiparameter identification of permanent magnet synchronous motors based on improved sparrow search algorithm," *New Technology of Electrical Energy*, Vol. 41, No. 05, 26–34, 2022.
8. Li, Y., X. Dong, H. Wei, et al., "Parameter identification of permanent magnet synchronous motors based on improved model reference adaptive systems," *Control Theory and Application*, Vol. 37, No. 09, 1983–1988, 2020.
9. Li, W. and Z. Du, "Parameter identification of permanent magnet synchronous motor based on improved grey wolf optimization algorithm," *Modular Machine Tool and Automatic Machining Technology*, Vol. 557, No. 07, 113–117, 2020.
10. Wu, Z., D. Yu, and X. Kang, "Parameter identification of solar cell models based on improved ant lion optimization algorithm," *Acta Energiae Solaris Sinica*, Vol. 40, No. 12, 3435–3443, 2019.

11. Liu, X., W. Hu, Y. Zou, et al., "Multi parameter identification of permanent magnet synchronous motors using improved particle swarm optimization," *Journal of Electrical Machinery and Control*, Vol. 24, No. 07, 112–120, 2020.
12. Türker, T., U. Buyukkeles, and A. F. Bakan, "A robust predictive current controller for PMSM drives," *IEEE Transactions on Industrial Electronics*, Vol. 63, No. 6, 3906–3914, 2016.
13. Wang, Z., A. Yu, X. Li, G. Zhang, and C. Xia, "A novel current predictive control based on fuzzy algorithm for PMSM," *IEEE Journal of Emerging and Selected Topics in Power Electronics*, 990–1001, 2019.
14. Siami, M., D. A. Khaburi, M. Rivera, and J. Rodriguez, "An experimental evaluation of predictive current control and predictive torque control for a PMSM fed by a matrix converter," *IEEE Transactions on Industrial Electronics*, Vol. 64, No. 11, 8459–8471, 2018.
15. El-Sousy, F. F. M., Hybrid-based wavelet-neural-network tracking control for permanent-magnet synchronous motor servo drives," *IEEE Transactions on Industrial Electronics*, Vol. 57, No. 9, 3157–3166, 2010.
16. Wang, Y., X. Wang, W. Xie, et al., "Deadbeat model-predictive torque control with discrete space-vector modulation for PMSM drives," *IEEE Transactions on Industrial Electronics*, Vol. 64, No. 5, 3537–3547, 2017.
17. Wu, C., Y. Zhao, and M. Sun, "Multi-parameter online identification of permanent magnet synchronous motors using measured voltages," *Proceedings of the CSEE*, Vol. 40, No. 13, 4329–4340, 2020.
18. Wang, G., "Current predictive control and current static error elimination algorithm for permanent magnet AC servo systems," Harbin Institute of Technology, 2014.
19. Naruei, I., F. Keynia, and A. Sabbagh Molahosseini, "Hunter-prey optimization: Algorithm and applications," *Soft Computing*, Vol. 26, 1279–1314, 2022.
20. Xue, J., "Research and application of a new swarm intelligence optimization technology," Donghua University, 2020.